

**Bioinspired photocatalytic hedgehog coating with liquid
repellency towards highly wetting fluids**

Journal:	<i>Materials Chemistry Frontiers</i>
Manuscript ID	QM-RES-02-2021-000325.R1
Article Type:	Research Article
Date Submitted by the Author:	05-Apr-2021
Complete List of Authors:	Sarma, Jyotirmoy; The University of Texas at Dallas, Mechanical Engineering Guo, Zongqi; The University of Texas at Dallas, Mechanical Engineering Dai, Xianming; The University of Texas at Dallas, Mechanical Engineering

ARTICLE

Bioinspired photocatalytic hedgehog coating for super liquid repellency

Jyotirmoy Sarma, Zongqi Guo and Xianming Dai*

Received 00th January 20xx,
Accepted 00th January 20xx

DOI: 10.1039/x0xx00000x

Super liquid repellency towards highly wetting liquids is of great interest for fundamental research and practical applications. Superomniphobic coatings have been made by forming re-entrant or doubly re-entrant morphologies that result in contact angles above 150° and contact angle hysteresis below 10° . While existing superomniphobic coatings rely on stringed nanoparticles to make re-entrant geometries, we show that a new type of superomniphobic surface is made by microscale hedgehog particles that combine the features of springtail inspired re-entrant microspheres with cicada wings inspired nanoneedles. Such a bioinspired hedgehog coating shows super liquid repellency from water to low surface tension liquids like dodecane with a surface tension of 25.3 mN m^{-1} . The hedgehog particles provide re-entrant structures and the nanoneedles minimize the local liquid-solid adhesion due to the presence of air gaps. Moreover, we use a one-step approach to make scalable titanium dioxide hedgehog coatings with the photocatalytic property. Thus, the photocatalytic hedgehog coating can be easily converted to slippery liquid-infused porous surfaces under ultraviolet illumination in one-step. Such a photocatalytically activated slippery surface shows an ultralow contact angle hysteresis ($\leq 1^\circ$) to highly wetting fluids with surface tensions as low as 16 mN m^{-1} .

1. Introduction

Liquid repellent coatings are being broadly studied to explore the fundamental interfacial phenomena¹⁻⁶, and due to their wide range of potential practical applications in self-cleaning⁷, drag reduction⁸, anti-corrosion⁹, anti-fouling¹⁰, fog harvesting¹¹, chemical shielding¹², thermal insulation¹³, and anti-/deicing¹⁴ to name a few. An ideal superomniphobic coating should ensure stable liquid repellency and should possess easy deposition through a simple process on substrates regardless of their size, shape, or composition. The overall performance of a liquid repellent coating is primarily dependent on the surface texture and surface chemistry. All these factors are interrelated; hence it is a complicated process to design a simple yet versatile superomniphobic coating. For a successful design, there has to be a coexistence of re-entrant curvature along with the surface chemistry and appropriate roughness^{1, 15}. This allows the liquid droplet resting on the surface to be in the Cassie-Baxter state¹⁶ maintaining an apparent contact angle (CA) larger than 150° , and a contact angle hysteresis (CAH) lower than 10° .

The re-entrant morphology on superomniphobic surfaces is inspired by the nanotextures found on the body of insects like springtail which keeps them non-wetted while coming in contact with oils. Most commonly, lithographic methods are used to fabricate re-entrant texture on flat silicon and complex geometries like wrinkled surfaces¹⁷, even replicating the springtail structure^{18, 19}. However, such superomniphobic surfaces based on silicon involve complex micro/nano

fabrication processes and are not scalable. Beyond silicon, re-entrant texture can be fabricated on surfaces to render them superomniphobic either through nanoparticle coating⁴, electrospinning of polymers¹², electrochemical etching²⁰, and polymerization of fluorosilanes^{21, 22} and medical-grade cyanoacrylates²³. Nanoparticulate superomniphobic coatings generally utilize stringed^{4, 24, 25} or modified nanoparticles²⁶ instead of discrete nanoparticles to create the re-entrant morphology. One such example is fumed silica which consists of tertiary particles formed by the agglomeration of stringed particles. This is because a coating made of simple spherical nanoparticles fails to repel liquids of low surface tensions²⁴. The liquid droplets get pinned on these surfaces due to an insignificant re-entrant structure resulting in large CAH. Consequently, all micro/nanoparticle-based superomniphobic surfaces to date have leveraged stringed micro/nanoparticles to form re-entrant texture for successful repellency of low surface tension liquids. Hierarchically structured superoleophobic surfaces can achieve ultralow CAH with ultralow roll-off angles for low surface tension liquids due to reduced solid-liquid contact area²⁷. A recent study reported a design strategy to create hierarchical micro/nano re-entrant texture by combining photolithography-based re-entrant microstructures with stringed nanoparticles²⁸. This hierarchical surface could repel liquids with surface tensions as low as 26.5 mN m^{-1} .

Department of Mechanical Engineering, The University of Texas at Dallas, 800 W. Campbell Rd., Richardson, Texas 75080, USA. Email: dai@utdallas.edu

Electronic Supplementary Information (ESI) available: Supplementary figures S1-6 show the liquid repellency property, hedgehog particle synthesis criteria, parametric optimization of hedgehog coating, self-cleaning and coalescence-induced jumping of low surface tension liquids. See DOI: 10.1039/x0xx00000x

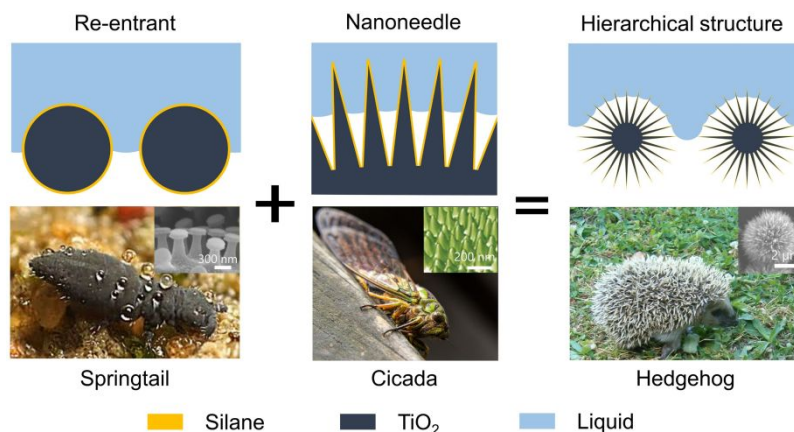


Figure 1. Schematic illustration for the design of hedgehog coating, i.e., a new superomniphobic surface that combines the springtail inspired re-entrant microspheres with cicada wings inspired nanoneedles. The hedgehog structure reduces the overall liquid/solid contact area compared with individual micro-reentrant surface or the nanoneedle surface alone because of the robust air-cushions. The image for springtail has been courtesy of B. Valentine, and related SEM image of re-entrant structure (inset) has been adapted from Ref [15]. © The Authors, some rights reserved; exclusive licensee AAAS. Distributed under a Creative Commons Attribution NonCommercial License 4.0 (CC BY-NC) <http://creativecommons.org/licenses/by-nc/4.0/>. The AFM image of nanoneedles has been adapted from Ref [25]. Cicada (Photo by FlyingPete at morguefile.com) and hedgehog (Photo by Erland at morguefile.com).

The presence of re-entrant curvature is not the only feasible solution for developing non-wetting surfaces. Insects like cicada's wings never get wet due to the presence of needle-like nanostructures on their wings^{29, 30}. Nucleation of water droplets occurs in the nanoneedle structure but does not wet the surface due to Laplace expulsion between the textures which makes the droplets move outwards. However, the non-wetting state vanishes above critical pressures which depend on the shape and size of the nanoneedles. Interestingly, this phenomenon is reversible only for conical shaped nanoneedles where the air gaps reappear spontaneously after depressurization³¹. However, the nanoneedle structure is only limited to repelling water, and cannot prevent liquid penetration into the structures when in contact with low surface tension liquids³². As such, if the liquid/solid surface area is increased, the nanoneedle structures are successful in repelling low surface tension liquids like hexadecane maintaining low interfacial adhesion, with a partial impregnation of the oil into the surface textures forming a penetration Cassie state^{32, 33}. Researchers utilized hydrothermal etching of metal oxides to fabricate coatings comprising of flower-like microparticles to repel liquids with low surface tensions, as low as 27.5 mN m^{-1} such as hexadecane^{34, 35}. These coatings rely on the re-entrant texture of the microparticles as well as the nanopetals/grooves to exhibit low solid/liquid adhesion. However, their performance for superomniphobicity was not quite satisfactory due to the lack of a proper design methodology of surface topography. These nanopetals/grooves must maintain a critical aspect ratio to have a non-wetting surface³⁶. The wetting mode on a V-shaped nanopetal/groove is determined by the intrinsic contact angle θ and the angle of V-shape β , and the criteria for non-wettability is such that $\beta < 2\theta - \pi$. Reducing the β value can further improve non-wettability.

In this work, we fabricate 'hedgehog'³⁷ shaped sub-micrometer titanium dioxide particles with a one-step hydrothermal method. The superomniphobic coating with hedgehog particles combines the re-entrant texture of a spherical microparticle with non-wetting characteristics of

conical nanoneedles to achieve ultralow liquid/solid adhesion by enabling hierarchical micro/nano- airgaps at the liquid/solid interface. We show that by re-designing the topography of a spherical microparticle with coordinated nanoneedles, the dependence of superomniphobicity on stringed nanoparticles can be mitigated. Furthermore, the hedgehog particles do not rely on ribbed nanoneedle arrays but can achieve stable liquid repellency with surface tensions ranging from 72.8 to 25.3 mN m^{-1} . This superomniphobic coating can readily be applied on various substrates like silicon, glass, wood, and cotton fabrics. In addition, because of the photocatalytic property of the TiO_2 and porous structure of this hedgehog coating, it can readily be converted to the slippery liquid infused porous surface (SLIPS) by infusion of silicone oil lubricant and UV light grafting in one step without the use of silane. This facile up-gradation results in enhanced liquid repellency performance, with even perfluorinated liquids like FC40 ($\gamma = 16 \text{ mN m}^{-1}$).

2. Experimental

2.1 Materials

Titanium (IV) chloride (98+ %), titanium (IV) n-butoxide (99+ %), toluene, diodomethane (99%, stabilized), n-hexadecane and n-dodecane (99%) purchased from VWR were used as received. Heptadecafluoro-1,1,2,2-tetrahydrodecyltrichlorosilane (FDTS) was purchased from Gelest Inc. Plain glass slides $5 \text{ cm} \times 2.5 \text{ cm} \times 0.1 \text{ cm}$ were purchased from Cornin. Wood and cotton wool were purchased from Office Depot and silicon wafers were purchased from University Wafers. Fumed silica (diameter 7 nm) powder was purchased from Sigma-Aldrich. Ethanol (70%) was purchased from AlphaTec. Iron (II, III) oxide powder (95%) was purchased from Sigma-Aldrich, and NeverWet® multi-surface water repellent coating spray was purchased from Amazon.

2.2 Synthesis of hedgehog particles

Titanium (IV) chloride was dissolved in deionized water in an ice-water bath under vigorous stirring to obtain a 50 wt. % aqueous TiCl_4 solution. Then, 4 mL of titanium (IV) n-butoxide

(TBT) was dissolved in 30 mL of toluene in an ice-water bath, and this was followed by dropwise addition of the aqueous TiCl_4 into the TBT/toluene solution under stirring. The stirring of the solution continued for 1 h, after which the mixture was transferred into a 50 mL stainless steel autoclave lined with Teflon and held at 180°C in the oven for 4 h. Eventually, the autoclave was rapidly cooled under tap water, followed by washing of the precipitates with ethanol several times to remove organic impurities and centrifuged to separate TiO_2 nanoparticles from the hierarchical hedgehog TiO_2 microparticles. The resulting hedgehog particles were kept dispersed in ethanol. The dispersion could also be held at 70°C in the oven for 12 h to obtain the dry hedgehog particles.

2.3 Fabrication of superomniphobic hedgehog coating

The glass and silicon substrates were washed with acetone and ethanol prior to use and dried under compressed dry air. A commercial organic binder (NeverWet[®]), comprising methyl isobutyl ketone, butyl acetate, and mineral spirits, was sprayed onto the substrates. The hedgehog particles dispersed in ethanol were then spin-coated immediately. The spin speed was fixed at 4000 rpm to obtain a uniform coating. This was followed by functionalization of the coated samples using ~ 100 μL of heptadecafluoro-1,1,2,2-tetrahydrodecyltrichlorosilane (FDTS), and kept for 12 h at room temperature. For all our experiments, spin-coated samples were used.

2.4 Contact angle measurements

The static contact angle and roll-off angle measurements were conducted using a Ramé-Hart 290-U1 standard goniometer. Contact angle measurements were implemented by advancing and receding a small droplet of liquid (~ 5 μL) onto the coated substrate using 3-5 individual measurements at different positions on each sample. A syringe was used for water droplet, and a pipette was used for all other low surface tension liquids. The roll-off angles were measured by tilting the goniometer stage until the droplet (~ 5 μL) started rolling off the substrate.

2.5 Characterization

The hedgehog particle coated surfaces were imaged by scanning electron microscopy (SEM) using a Zeiss Supra 40 scanning electron microscope at 15 kV.

2.6 High-speed imaging

Droplet dynamics videos for coalescence-induced jumping of low surface tension liquid droplets were obtained using a Photron Fastcam SA4 high-speed camera at 3600 frames per second.

3. Results and discussion

3.1 Bioinspired design and wettability of the hedgehog coating

In this study, we report the design rationale for a superomniphobic coating that combines the springtail inspired micro re-entrant texture with cicada wings inspired conical nanoneedles to form the hierarchical hedgehog microparticle (**Figure 1**). This unique hedgehog structure consolidates the re-entrant texture at the microscale and solidifies the air gaps at the nanoscale. Consequently, the solid/liquid interactions at the interface are substantially achieved. Titanium dioxide (TiO_2) has been used as the material in our study owing to its photocatalytic property. It is also widely used in different coating applications like painting, dip- and spray coating.

Superomniphobic coatings in previous studies avoided the use of particles without any branched structure because they could not repel low surface tension oils due to the lack of appropriate re-entrant or overhang textures. A comparison of nanoparticles, stringed nanoparticles, and hedgehog particles has been demonstrated in **Figure 2a**. The SEM images of the corresponding surface morphologies are presented in **Figure 2b** with inset images of a droplet of dodecane resting on them, respectively. For water, each of the three coatings showed superhydrophobicity with contact angles of $157 \pm 3^\circ$, $162 \pm 2^\circ$, and $165 \pm 1^\circ$, and CAH of $10 \pm 2^\circ$, $5 \pm 1^\circ$, and $3.5 \pm 0.5^\circ$, respectively. While nanoparticles showed a slightly larger CAH, stringed nanoparticles and hedgehog particles are both non-wetting to water droplets. However, nanoparticles failed to repel the low surface tension liquid of dodecane ($\gamma = 25.3$ mN m^{-1}). It showed a CA of $142 \pm 2.5^\circ$ and CAH above 20° for

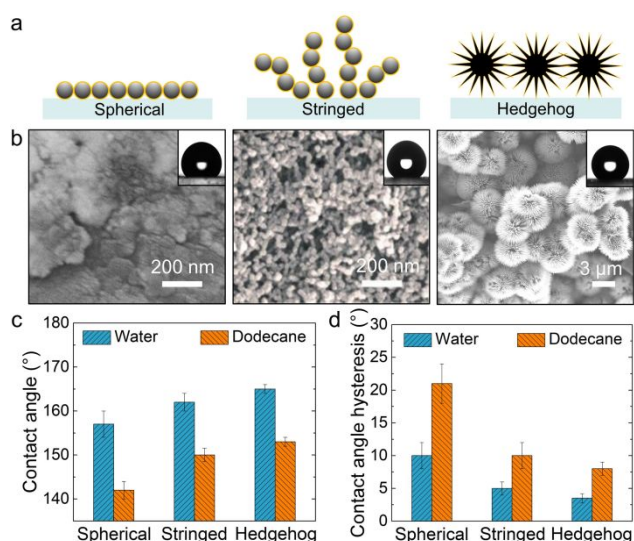


Figure 2. Superomniphobic hedgehog coating. **a.** Schematic illustration of spherical, stringed nanoparticles and hedgehog particles. The yellow colour denotes fluorosilane. **b.** SEM images of spherical, stringed nanoparticles (re-used from Ref [20]) and hedgehog particles. Inset: A droplet of dodecane resting on each of the three surfaces. **c.** Contact angles of water and dodecane on the three surfaces. **d.** Contact angle hysteresis of water and dodecane on the three surfaces.



Figure 3. Synthesis of hedgehog particles. **a.** Schematic illustration of the hydrothermal synthesis process for the hedgehog particles. **b.** SEM images of the final product showing the individual particle. Stirring time **c.** 1 min, **d.** 30 min, and **e.** 60 min, while keeping the other parameters the same, e.g., the reaction temperature, reaction time and precursor ratio of TBT:TiCl₄ at 180°C, 4 h, and 1:0.65, respectively. Scale bar: 2 μm.

dodecane droplets (**Figure 2c**). On the contrary, stringed nanoparticle coating fabricated with fumed silica showed a CA of $150 \pm 2^\circ$ with the corresponding hysteresis around 10° . Meanwhile, the hedgehog particle coating repelled dodecane quite easily with a CA of $153 \pm 1^\circ$ and CAH $8 \pm 1^\circ$. Hence, coatings made of both stringed nanoparticles and hedgehog particles were superomniphobic towards liquids of surface tension as low as 25.3 mN m^{-1} , and the hedgehog particles perform even better. This demonstrates that if spherical particles are re-designed to have nanoscale air gaps and appropriate re-entrant texture, then coatings with such particles have comparable or better liquid repellency compared to coatings with existing stringed nanoparticles. This shed new light on the fabrication of superomniphobic surfaces.

3.2 Synthesis of hedgehog particles and fabrication of superomniphobic coatings

The scalable and one-step synthesis of the hierarchical hedgehog particles takes place in a hydrothermal process (**Figure 3a**) with the influence of different reaction conditions including the ratio of reactants, reaction time, reaction temperature and concentration of reactants on the morphology and the size of the particles³⁸. Titanium (IV) chloride was dissolved in deionized water in an ice-water bath under vigorous stirring to obtain a 50 wt. % aqueous TiCl₄ solution. Then, 4 mL of titanium (IV) n-butoxide (also known as tetrabutyl titanate) (TBT) was dissolved in 30 mL of toluene in the ice-water bath, and this was followed by a dropwise addition of the aqueous TiCl₄ into the TBT/toluene solution under stirring. The stirring of the solution continued for 1 h, during which precipitation occurred at the bottom of the container. It is important that after 1 h of stirring, the mixture along with the precipitates was transferred into a 50 mL stainless steel autoclave that was lined with Teflon and held at 180°C in the oven for 4 h. Eventually, the autoclave was rapidly cooled under tap water to stop the further reaction, followed by washing the final precipitates with ethanol several times to remove any organic impurities and centrifuged to separate the hierarchical hedgehog TiO₂ microparticles from the nanoparticles in the mixture. The morphology of the hedgehog coating and a single hedgehog particle is demonstrated through the scanning electron microscopy (SEM) images in **Figure 3b**. The diameter of

a single hedgehog TiO₂ microparticle synthesized at 180°C for 4 h is in the range of 3-5 μm, with the nanoneedles growing radially from the core of the microspheres.

The precursor ratio of reactants, reaction time, and reaction temperature were changed during the syntheses to investigate the influence of different reaction conditions and understand the formation mechanism of the hierarchical TiO₂ microspheres. Changing the reaction time can have a change in the morphology of the hedgehog microparticles. When the temperature is kept constant at 180°C for the hydrothermal reaction process for 2 h duration, 3D hierarchical hedgehog microspheres are developed as shown in **Figure S1a**. However, when the reaction process time is increased to 4 h at a constant reaction temperature of 180°C, the hedgehog microparticles show a more uniform structure as compared to the 2 h synthesis time (**Figure S1b**). The precursor ratio of TBT to TiCl₄ plays a significant role in the morphology of the hedgehog microparticles. When the ratio of TBT:TiCl₄ is 1:1.30, keeping the reaction temperature and reaction time constant at 180°C and 4 h, the resulting hedgehog particles are in the diameter range of 1-2 μm as shown in **Figure S2a**. These particles have hierarchical nanoneedles but do not represent the hedgehog structure as the nanoneedles are much thicker in shape. However, by decreasing the concentration of TiCl₄ and changing the ratio of TBT:TiCl₄ to 1:0.65 and keeping the other reaction conditions constant, hedgehog microparticles with 3D structures are obtained as shown in **Figure S2b**. The diameters of these microparticles are in the range of 3-5 μm. Another important thing to account for during the stirring of the aqueous TiCl₄ into the TBT/toluene mixture is the formation of the precipitate at the bottom of the container. We compared three different sample mixtures for studying the influence of the precipitate. The first sample was prepared by stirring the solution mixture for just 1 minute, the second sample was prepared by stirring the mixture for 30 minutes, and for the third sample, the solution mixture was stirred for 1 h, and then the three samples were transferred into the autoclave and kept in the oven at a reaction temperature of 180°C and a reaction time of 4 h. Finally, the results can be observed as shown

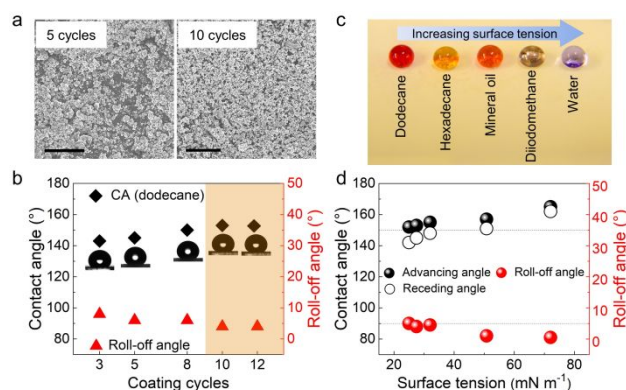


Figure 4. Parametric optimization of the hedgehog coating. **a.** SEM images of 5 and 10 spin-coating cycles. Scale bar: 100 μm. **b.** The contact angles and the corresponding roll-off angles for dodecane ($\gamma = 25.3 \text{ mN m}^{-1}$) with varying coating cycles. 10 coating cycles and above established uniform particle coverage rendering superoleophobicity which is shown in highlighted color. **c.** Dyed liquid droplets with increasing surface tension are resting on a silane-coated hedgehog surface. **d.** The repellency of liquids with various surface tensions ($\gamma = 25.3\text{-}72.8 \text{ mN m}^{-1}$) on the hedgehog coating representing excellent superomniphobicity.

through the SEM images in **Figure 3c, d** and **e** where the 1-minute stir produced a morphology of star-shaped microparticles with a diameter range of 1-2 μm , the 30-minute stir produced a morphology of microspheres and hierarchical nanospikes having a diameter of 2 μm approximately. The hierarchical nanospikes were not densely populated and lacked uniformity. While the 1 h stir produced the morphology of hedgehog particles with hierarchical nanoneedles which best resembles the hedgehog shape with an average diameter in the range of 3-5 μm . The final products from the three stirring times were tested for repellency towards dodecane ($\gamma = 25.3 \text{ mN m}^{-1}$) where only the hedgehog particles from the 1 h stir condition showed complete repellency with contact angle above 150° and hysteresis below 10° (**Figure S3**). The process of ethanol wash and centrifugation after taking out the product from the autoclave is quite important as it helps to get rid of TiO_2 nanoparticles formed during the process, which can usually occupy the gaps between the nanoneedles as shown in **Figure S4**. With this, we conclude that the reaction temperature, reaction time and precursor ratio can be varied to control the overall size and morphology of the hedgehog particles. The morphology of the hedgehog particles is the optimal when the precursor ratio of the reactants is 1:0.65, stirring is continued for 1 h, the reaction temperature is set at 180°C , and the reaction is 4 h in the oven.

The synthesized hedgehog particles are hydrophilic in nature and can be dispersed well in 70% pure ethanol. The dispersion of hydrophilic hedgehog particles in ethanol is then spin- or dip-coated onto a substrate to form a uniform coating. The bonding of the particles to the substrate is facilitated using an organic binder comprising methyl isobutyl ketone, butyl acetate, and mineral spirits. This is followed by the functionalization of the coating using fluorosilane to lower its surface energy. The hedgehog coating can be scalable as it can be sprayed or dip-coated on to substrates. However, several layers might be necessary to achieve appropriate superomniphobicity.

3.3 Parametric optimization of hedgehog coating

The hedgehog coating with a 1-cycle spin coating at 5000 rpm followed by fluorosilanization yielded a superhydrophobic surface with a water contact angle of 163° and hysteresis 3.5° . A Wenzel state was observed in the case of dodecane with a contact angle of 142° , and the droplet was pinned because the substrate was not covered uniformly by hedgehog particles. This could be overcome with multiple spin-coating cycles to

attain a surface with uniform particle coverage (**Figure S5a, b** and **c**). The SEM images in **Figure 4a** show the surface coverage of hedgehog particles after 5 and 10 spinning cycles. We found that after spin-coating of 8 cycles the hedgehog coating turned superomniphobic towards dodecane with CA just above 150° (**Figure 4b**). Further spin coating up to 10 cycles saw the dodecane CA rise to 153° with droplet rolling angle below 5° , and remained consistent after 12 cycles of spinning. Hence, a hedgehog coating with 10 spinning cycles was taken as a standard for all subsequent tests. The fabricated hedgehog coating with unique re-designing of the primary particle having hierarchical re-entrant nanoneedle textures was rendered to be a superomniphobic surface that repels liquids of various surface tension ranging from water ($\gamma = 72.8 \text{ mN m}^{-1}$) to dodecane ($\gamma = 25.3 \text{ mN m}^{-1}$) as shown in **Figure 4c, d**. The contact angle hysteresis value for dodecane was $8 \pm 1^\circ$, and the roll-off angle was measured to be 5° .

Liquid repellent coatings are highly desired for solar panels, buildings, and vehicles due to their self-cleaning property. The superomniphobic hedgehog coating can exhibit excellent self-cleaning property as demonstrated in **Figure S6a**, where iron oxide powders, imitated as dust contaminants, are removed by impacting water droplets without leaving any dust residue on the surface. The hedgehog coating also shows good performance in coalescence-induced jumping of low surface tension droplets. As shown in **Figure S6b**, two droplets of an ethanol-water mixture ($\gamma = 47.6 \text{ mN m}^{-1}$) of 5 μL volume each are made to coalesce with each other, resulting in successful induced jumping of the coalesced droplets of low surface tension. The hedgehog coating with characteristics of self-cleaning and induced jumping of low surface tension droplets is versatile and substrate-independent as it can be applied on various surfaces like glass, silicon, and wood (**Figure 5**), and we demonstrated that water, as well as low surface tension liquid like dodecane, can easily roll off from the surface with a tilting angle as low as 5° .

For the purpose of liquid repellency, there is no durability issue of the hedgehog coating as such. The surface is superomniphobic towards dodecane ($\gamma = 25.3 \text{ mN m}^{-1}$) even after 3 months of fabrication of the coating. However, the superomniphobic performance would not be sustainable if the surface gets abraded. This is because the texture of the hedgehog particles would be damaged due to breakage of the nanoneedles.

3.4 Facile one-step conversion of hedgehog coating to SLIPS

The hedgehog TiO_2 coating can be easily converted to a slippery liquid infused porous surface (SLIPS) using a one-step strategy. SLIPS is a state-of-the-art liquid repellent surface, where the air lubricant within the porous structure is replaced with a liquid lubricant and is well known for its omniphobic nature with very low contact angle hysteresis ($< 2.5^\circ$)³. The existing method for fabrication of a conventional SLIPS involves a couple of steps starting with functionalization of a porous/textured surface, followed by its impregnation with low surface energy, chemically inert lubricant to form a physically smooth and chemically homogeneous surface as shown in the schematic in **Figure 6a**. The functionalization step, which takes at least 4 h, is done to lower the surface energy of the porous texture so that a low surface tension lubricant can be immobilized stably within the surface texture.

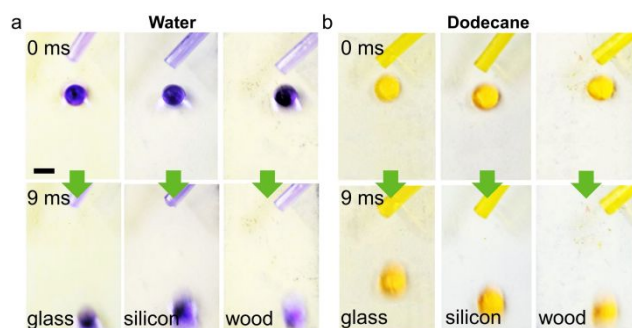


Figure 5. Substrate-independent superomniphobic hedgehog coating. Pictures showing hedgehog coating on various substrates such as glass, silicon and wood which have successful repellency towards **a.** water, and **b.** dodecane. 20 μL droplet is used. Scale bar: 2 mm.

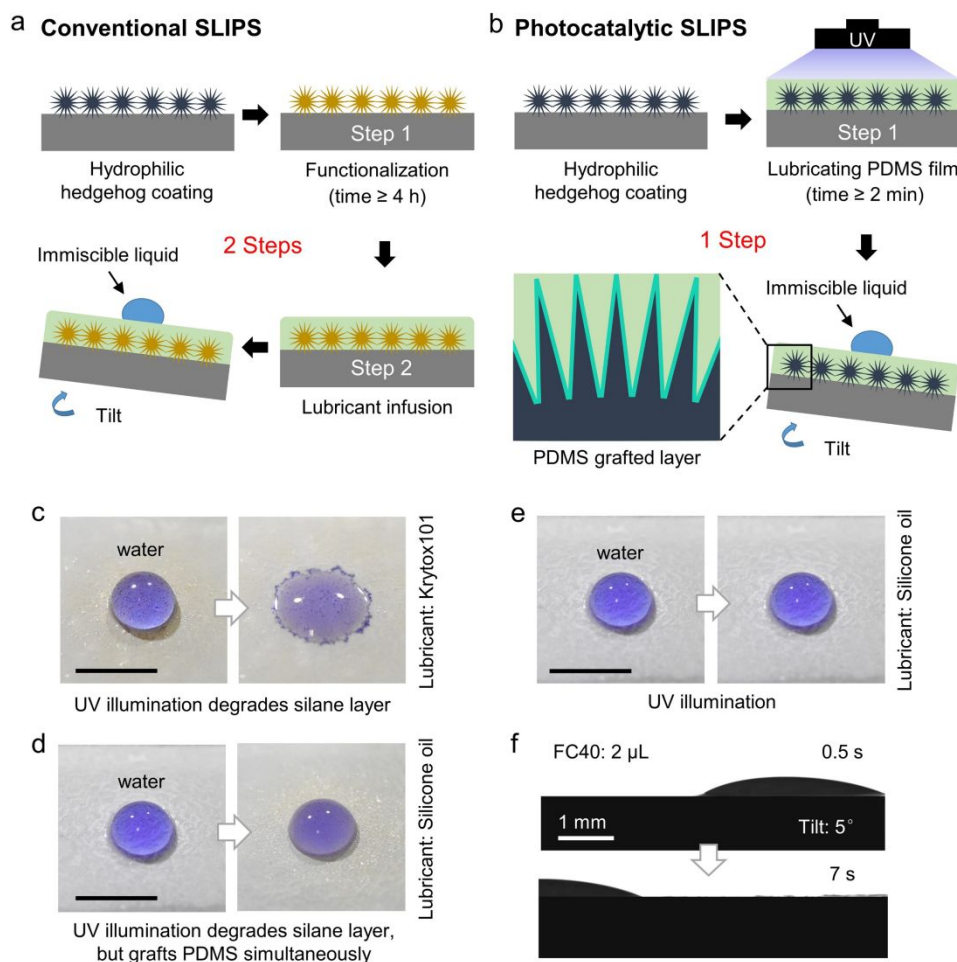


Figure 6. Facile one-step fabrication of photocatalytic SLIPS. Schematic showing fabrication steps for **a.** conventional SLIPS and **b.** photocatalytic SLIPS. Photocatalytic SLIPS is made by simultaneous infusion of silicone oil onto hydrophilic hedgehog surface and UV light grafting of PDMS molecular chains within 2 minutes which render the surface to be hydrophobic. **c.** UV illumination (15 min) of conventional SLIPS with fluoroalkyl silane and Krytox101 lubricant lost water repellency. 20 μL water droplet dyed in blue wets the surface. **d.** UV illumination (15 min) of conventional SLIPS with fluoroalkyl silane hydrophobic layer and silicone oil lubricant maintained its water repellency. **e.** UV illumination (15 min) of photocatalytic SLIPS maintained water repellency. Scale bar for **c, d, e:** 1 cm. **f.** One-step photocatalytic SLIPS results in liquid repellency to perfluorinated liquids like FC40 ($\gamma = 16 \text{ mN m}^{-3}$).

Recent studies have shown that poly(dimethylsiloxane) (PDMS) can be grafted as polymer brush on the surface of metal-oxide photocatalysts from silicone oil (methyl-terminated PDMS) under illumination^{39, 40}. Titanium dioxide is well known for its photocatalytic property, and we have utilized this property to fabricate photocatalytic SLIPS. In a one-step process, we impregnate the bare hedgehog TiO_2 coating with trimethylsiloxy-terminated PDMS (viscosity: 200 cSt) and simultaneously illuminate with UV light so that PDMS is grafted to the surface of the TiO_2 hedgehog particles and the excess liquid PDMS acts as the infused lubricant (**Figure 6b**). The grafting is realized within 2 minutes with a UV light of 365 nm wavelength when the distance between the light source and the sample is within 5 cm. The grafted PDMS brushes act as the hydrophobic functionalized layer. Methyl-terminated PDMS has been selected due to its high thermal stability arising from the large bond energy (452 kJ mol^{-1}), as well as its inherent low surface energy from the hydrophobic methyl side groups. The liquid lubricant remains stably locked within the hydrophobic layer because they both are chemically the same. The fabrication of photocatalytic SLIPS is facile not only because of

the one-step process but also due to the significant reduction in time required for functionalization and is cost-effective.

The photocatalytic property of metal oxide photocatalysts like TiO_2 can degrade organic compounds like fluoroalkyl silanes when illuminated under UV light, due to the generation of free radicals which react with molecules of the organic compounds. Hence, conventional SLIPS with metal-oxide photocatalyst based porous texture cannot be utilized for applications directly under sunlight as it will lose its liquid repellent property due to decomposition of the functionalized hydrophobic layer. A conventional SLIPS that consisted of TiO_2 hedgehog particles as a base layer with FDTs silane as the hydrophobic layer along with Krytox101 as the lubricant, lost its liquid repellency within 15 min of UV illumination and was rendered hydrophilic (**Figure 6c**). However, it was noted as shown in **Figure 6d** that if the lubricant is changed to silicone oil in the conventional SLIPS, its liquid repellency is mostly maintained even after UV illumination. The fact is that UV illumination decomposes the fluoroalkyl silane layer, but eventually starts grafting PDMS hydrophobic layer. Hence, to keep things simple and cost-effective, by using a photocatalytic hedgehog SLIPS instead of a conventional SLIPS, the liquid repellency property can be kept

intact even after long durations of UV illumination (**Figure 6e**). With the successful fabrication of the photocatalytic hedgehog SLIPS, the surface now showed an enhanced liquid repellency by repelling perfluorinated liquids like FC40 with surface tensions as low as 16 mN m^{-1} (**Figure 6f**) with a tilting angle of the substrate no more than 5° and achieving an ultralow contact angle hysteresis ($\leq 1^\circ$). This forms a one-step approach to fabricate a stable photocatalytic hedgehog SLIPS that repels highly wetting liquids, such as FC40.

Conclusions

We have developed a multifunctional hedgehog particle with photocatalytic functionality that can repel liquids from water to FC40. We have put forward a new design strategy for developing a superomniphobic coating by combining the micro re-entrant textures surrounded with nanoneedle structures, i.e., hedgehog coating. This methodology introduces nano-airgaps with reduced liquid-solid interactions leading to an excellent liquid repellency with low contact angle hysteresis to low surface tension liquids like dodecane ($\gamma = 25.3 \text{ mN m}^{-1}$). This represents a new design rationale when most superomniphobic coatings rely on stringed nanoparticles. By changing the air lubricant to liquid lubricant, the liquid repellency can be enhanced significantly with repellency even to perfluorinated liquids (e.g., FC40) by a one-step conversion of the hydrophilic hedgehog coating to SLIPS through lubricant infusion and simultaneous UV illumination, which promotes grafting of PDMS polymer brushes utilizing the photocatalytic property of the hedgehog TiO_2 particles. We envision that our

superomniphobic coating can further be studied to improve the durability and explore potential applications, such as anti-corrosion, anti-fouling, etc.

Author Contributions

X.D. conceived the idea and supervised the research. J.S. and X.D. designed the experiments. J.S. and Z.G. synthesized the hedgehog particles and performed characterization. J.S. performed the experiments. All authors discussed the results, conducted the data analysis, and wrote the manuscript. All authors have approved the final version of the manuscript.

Conflicts of interest

There are no conflicts of interest to declare.

Acknowledgments

The authors gratefully acknowledge the startup funding support (Grant No. 40030467) by the University of Texas at Dallas (UT Dallas), National Science Foundation in the United States (Award No. 1929677), and the Young Investigator Program at Army Research Office (Award No. W911NF1910416). J.S. is grateful to Yang Han for his help on the initial synthesis of the hedgehog particles and for discussion with Lei Zhang. This project was partially funded by the Office of Research at UT Dallas through the Core Facility Voucher Program.

Notes and references

1. A. Tuteja, W. Choi, M. Ma, J. M. Mabry, S. A. Mazzella, G. C. Rutledge, G. H. McKinley and R. E. Cohen, Designing Superoleophobic Surfaces, *Science*, 2007, **318**, 1618-1622.
2. T. L. Liu and C.-J. C. Kim, Turning a surface superrepellent even to completely wetting liquids, *Science*, 2014, **346**, 1096-1100.
3. T.-S. Wong, S. H. Kang, S. K. Y. Tang, E. J. Smythe, B. D. Hatton, A. Grinthal and J. Aizenberg, Bioinspired self-repairing slippery surfaces with pressure-stable omniphobicity, *Nature*, 2011, **477**, 443-447.
4. X. Deng, L. Mammen, H.-J. Butt and D. Vollmer, Candle Soot as a Template for a Transparent Robust Superamphiphobic Coating, *Science*, 2012, **335**, 67-70.
5. L. Zhang, A. G. Zhou, B. R. Sun, K. S. Chen and H.-Z. Yu, Functional and versatile superhydrophobic coatings via stoichiometric silanization, *Nat. Commun.*, 2021, **12**, 982.
6. S. Wang, K. Liu, X. Yao and L. Jiang, Bioinspired Surfaces with Superwettability: New Insight on Theory, Design, and Applications, *Chem. Rev.*, 2015, **115**, 8230-8293.
7. Y. Lu, S. Sathasivam, J. Song, C. R. Crick, C. J. Carmalt and I. P. Parkin, Robust self-cleaning surfaces that function when exposed to either air or oil, *Science*, 2015, **347**, 1132-1135.
8. C. Lee and C.-J. Kim, Underwater Restoration and Retention of Gases on Superhydrophobic Surfaces for Drag Reduction, *Phys. Rev. Lett.*, 2011, **106**, 014502.
9. T. Xiang, Y. Han, Z. Guo, R. Wang, S. Zheng, S. Li, C. Li and X. Dai, Fabrication of inherent anticorrosion superhydrophobic surfaces on metals, *ACS Sustain. Chem. Eng.*, 2018, **6**, 5598-5606.
10. A. K. Epstein, T.-S. Wong, R. A. Belisle, E. M. Boggs and J. Aizenberg, Liquid-infused structured surfaces with exceptional anti-biofouling performance, *Proc. Natl. Acad. Sci. U. S. A.*, 2012, **109**, 13182-13187.
11. X. Dai, N. Sun, S. O. Nielsen, B. B. Stogin, J. Wang, S. Yang and T.-S. Wong, Hydrophilic directional slippery rough surfaces for water harvesting, *Sci. Adv.*, 2018, **4**, eaaq0919.
12. S. Pan, A. K. Kota, J. M. Mabry and A. Tuteja, Superomniphobic Surfaces for Effective Chemical Shielding, *J. Am. Chem. Soc.*, 2013, **135**, 578-581.
13. Z. Shao, Y. Wang and H. Bai, A superhydrophobic textile inspired by polar bear hair for both in air and underwater thermal insulation, *Chem. Eng. J.*, 2020, **397**, 125441.
14. M. J. Kreder, J. Alvarenga, P. Kim and J. Aizenberg, Design of anti-icing surfaces: smooth, textured or slippery?, *Nat. Rev. Mater.*, 2016, **1**, 1-15.
15. A. Tuteja, W. Choi, J. M. Mabry, G. H. McKinley and R. E. Cohen, Robust omniphobic surfaces, *Proc. Natl. Acad. Sci. U. S. A.*, 2008, **105**, 18200-18205.
16. A. Cassie and S. Baxter, Wettability of porous surfaces, *Trans. Faraday Soc.*, 1944, **40**, 546-551.
17. G.-T. Yun, W.-B. Jung, M. S. Oh, G. M. Jang, J. Baek, N. I. Kim, S. G. Im and H.-T. Jung, Springtail-inspired superomniphobic surface with extreme pressure resistance, *Sci. Adv.*, 2018, **4**, eaat4978.

18. S. M. Kang, J. S. Choi and J. H. An, Reliable and Robust Fabrication Rules for Springtail-Inspired Superomniphobic Surfaces, *ACS Appl. Mater. Interfaces*, 2020, **12**, 21120-21126.
19. S. Dong, X. Zhang, Q. Li, C. Liu, T. Ye, J. Liu, H. Xu, X. Zhang, J. Liu, C. Jiang, L. Xue, S. Yang and X. Xiao, Springtail-Inspired Superamphiphobic Ordered Nanohoodoo Arrays with Quasi-Doubly Reentrant Structures, *Small*, 2020, **16**, 2000779.
20. J. Song, S. Huang, K. Hu, Y. Lu, X. Liu and W. Xu, Fabrication of superoleophobic surfaces on Al substrates, *J. Mater. Chem. A*, 2013, **1**, 14783-14789.
21. J. Zhang and S. Seeger, Superoleophobic Coatings with Ultralow Sliding Angles Based on Silicone Nanofilaments, *Angew. Chem. Int. Ed.*, 2011, **50**, 6652-6656.
22. J. Zhang, B. Yu, Q. Wei, B. Li, L. Li and Y. Yang, Highly transparent superamphiphobic surfaces by elaborate microstructure regulation, *J. Colloid Interface Sci.*, 2019, **554**, 250-259.
23. N. Akhtar, P. J. Thomas, B. Svardal, S. Almendingen, E. d. Jong, S. Magnussen, P. R. Onck, M. A. Fernø and B. Holst, Pillars or Pancakes? Self-cleaning surfaces without coating, *Nano Lett.*, 2018, **18**, 7509-7514.
24. D. Ge, L. Yang, Y. Zhang, Y. Rahmawan and S. Yang, Transparent and Superamphiphobic Surfaces from One-Step Spray Coating of Stringed Silica Nanoparticle/Sol Solutions, *Part. Part. Syst. Char.*, 2014, **31**, 763-770.
25. H. Teisala, F. Geyer, J. Haapanen, P. Juuti, J. M. Mäkelä, D. Vollmer and H.-J. Butt, Ultrafast Processing of Hierarchical Nanotexture for a Transparent Superamphiphobic Coating with Extremely Low Roll-Off Angle and High Impalement Pressure, *Adv. Mater.*, 2018, **30**, 1706529.
26. Y. Akkus, A. Koklu and A. Beskok, Atomic Scale Interfacial Transport at an Extended Evaporating Meniscus, *Langmuir*, 2019, **35**, 4491-4497.
27. A. K. Kota, Y. Li, J. M. Mabry and A. Tuteja, Hierarchically Structured Superoleophobic Surfaces with Ultralow Contact Angle Hysteresis, *Adv. Mater.*, 2012, **24**, 5838-5843.
28. X. Li, D. Wang, Y. Tan, J. Yang and X. Deng, Designing Transparent Micro/Nano Re-Entrant-Coordinated Superamphiphobic Surfaces with Ultralow Solid/Liquid Adhesion, *ACS Appl. Mater. Interfaces*, 2019, **11**, 29458-29465.
29. T. Mouterde, G. Lehoucq, S. Xavier, A. Checco, C. T. Black, A. Rahman, T. Midavaine, C. Clanet and D. Quéré, Antifogging abilities of model nanotextures, *Nat. Mater.*, 2017, **16**, 658.
30. K. M. Wisdom, J. A. Watson, X. Qu, F. Liu, G. S. Watson and C.-H. Chen, Self-cleaning of superhydrophobic surfaces by self-propelled jumping condensate, *Proc. Natl. Acad. Sci. U.S.A.*, 2013, **110**, 7992-7997.
31. A. Checco, B. M. Ocko, A. Rahman, C. T. Black, M. Tasinkevych, A. Giacomello and S. Dietrich, Collapse and Reversibility of the Superhydrophobic State on Nanotextured Surfaces, *Phys. Rev. Lett.*, 2014, **112**, 216101.
32. X. Yao, J. Gao, Y. Song and L. Jiang, Superoleophobic Surfaces with Controllable Oil Adhesion and Their Application in Oil Transportation, *Adv. Funct. Mater.*, 2011, **21**, 4270-4276.
33. X. Yao, Q. Chen, L. Xu, Q. Li, Y. Song, X. Gao, D. Quéré and L. Jiang, Bioinspired Ribbed Nanoneedles with Robust Superhydrophobicity, *Adv. Funct. Mater.*, 2010, **20**, 656-662.
34. G. Perry, Y. Coffinier, V. Thomy and R. Boukherroub, Sliding Droplets on Superomniphobic Zinc Oxide Nanostructures, *Langmuir*, 2012, **28**, 389-395.
35. S. Movafaghi, W. Wang, A. Metzger, D. D. Williams, J. D. Williams and A. K. Kota, Tunable superomniphobic surfaces for sorting droplets by surface tension, *Lab on a Chip*, 2016, **16**, 3204-3209.
36. W. Xu, Z. Lan, B. L. Peng, R. F. Wen and X. H. Ma, Effect of nano structures on the nucleus wetting modes during water vapour condensation: from individual groove to nano-array surface, *RSC Advances*, 2016, **6**, 7923-7932.
37. J. H. Bahng, B. Yeom, Y. Wang, S. O. Tung, J. D. Hoff and N. Kotov, Anomalous dispersions of 'hedgehog' particles, *Nature*, 2015, **517**, 596-599.
38. L. Xiang, X. Zhao, J. Yin and B. Fan, Well-organized 3D urchin-like hierarchical TiO₂ microspheres with high photocatalytic activity, *J. Mater. Sci.*, 2012, **47**, 1436-1445.
39. S. Wooh, N. Encinas, D. Vollmer and H.-J. Butt, Stable Hydrophobic Metal-Oxide Photocatalysts via Grafting Polydimethylsiloxane Brush, *Adv. Mater.*, 2017, **29**, 1604637.
40. S. Wooh and H.-J. Butt, A Photocatalytically Active Lubricant-Impregnated Surface, *Angew. Chem. Int. Ed.*, 2017, **56**, 4965-4969.